

Beam Divergence Reduction Using Dielectric Lens for Orbital Angular Momentum Wireless Communications

Hiroyuki Fukumoto, Hirofumi Sasaki, Doohwan Lee, and Tadao Nakagawa

NTT Network Innovation Laboratories, NTT Corporation, 1-1 Hikarinooka, Yokosuka-shi, Kanagawa, Japan.

Abstract – In wireless communication systems that use radio beams carrying orbital angular momentum (OAM), beam divergence reduces the receiving signal power. To address this problem, we propose an antenna and dielectric lens arrangement method based on well-known optical imaging theory. We show the effectiveness of the proposed method by numerical analysis of the diffraction pattern for a finite aperture lens.

Index Terms —Orbital Angular Momentum (OAM), Beam Divergence, Optical Imaging Theory

1. Introduction

Wireless communication systems using radio beams carrying orbital angular momentum (OAM) are seen as a promising spatial multiplexing technique [1]. Each OAM mode has an orthogonal phase distribution on the wave front, thus, several OAM modes can be multiplexed coaxially.

Several OAM beam generation methods have been proposed [1-4]. Among them, Uniform-Circular-Array (UCA) is considered as one of promising candidates since UCA can transmit multiple OAM modes simultaneously [2,4].

The radiation pattern of OAM beams possesses two characteristics [5]: One is intensity nulls along the beam axis. The other is that the main-lobe direction varies with OAM mode. These characteristics, often referred to as OAM beam divergence, cause two problems. One problem is the existence of regions where the intensity becomes extremely low. As shown in Fig. 1(a), OAM beam intensity approaches zero in the region around the beam axis. Also, the region proportionally expands with the propagation distance of the OAM beam. Thus, a receiving antenna with limited size cannot receive the OAM beam properly [6]. The other is the mode-dependency of the position of maximum intensity. The degree of divergence angle becomes larger with OAM mode value, consequently, the radial position where the maximum intensity is obtained varies with OAM mode as shown in Fig. 1(b) [7]. As a result, when using some types of receiving antennas including UCA, the received power varies with OAM mode. In order to overcome these problems, it is necessary to reduce the divergence angle as well as to harmonize the angle of all OAM modes.

Although the simplest way to reduce the divergence angle is to expand UCA radius [4,5], the energy loss due to side lobes becomes excessive [4,5]. Moreover, when transmitting several OAM modes whose divergence angles are the same, one UCA is needed for each OAM mode used [5].

In this paper, we propose an antenna and lens arrangement method based on optical imaging theory. The proposed method can prevent OAM beam divergence.

2. Proposed Antenna and Lens Arrangement Method

Fig. 2 shows the proposed antenna and dielectric lens configuration. The UCA transmitting (Tx) antenna has N antenna elements uniformly distributed on the circumference

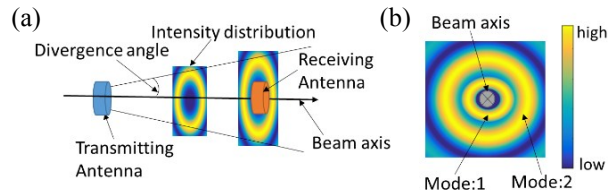


Fig. 1 Conceptual draw of OAM beam divergence.

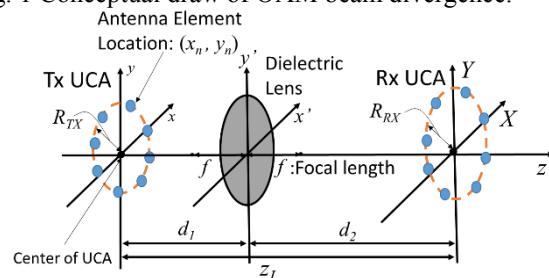


Fig. 2 Proposed antennas and lens arrangement.

of a circle with radius R_{TX} . The UCA receiving (Rx) antenna has radius R_{RX} . Tx and Rx antennas are installed on planes perpendicular to z -axis and they are arranged facing one another with spaces z_L . UCA Tx generates OAM-carrying beams that propagate along the z -axis [4].

In the proposed method, an optical imaging system is constructed by installing a thin dielectric lens between Tx and Rx UCAs. Through the optical imaging system, the OAM beam at the transmitted position is projected onto the Rx position as a “real image”. Thus, the problems associated with beam divergence are avoided at the Rx position. Here, we design the position and focal length of the dielectric lens the real image size equals UCA Rx size. First, we confirm the well-known thin-lens formula given by $1/d_1 + 1/d_2 = 1/f$, where, d_1 is object distance from UCA Tx to the lens, d_2 is image distance from the lens to UCA Rx, and f is the focal length. The magnification of the real image is given by d_2/d_1 . Also, the magnification should be related by $d_2/d_1 = R_{RX}/R_{TX}$. By using this relationship and the thin-lens formula, d_1 , d_2 and f are determined by

$$d_1 = \frac{R_{TX}}{R_{TX} + R_{RX}} z_L, d_2 = z_L - d_1, f = d_1 \left(1 - \frac{d_1}{z_L} \right). \quad (1)$$

Using (1) to design the thin lens reduces the effects of OAM beam divergence at the Rx position.

3. Derivation of Diffraction Pattern

In this section, we derive the diffraction pattern at the Rx position taking the impact of the finite aperture lens into consideration. First, we give a mathematical expression of the electromagnetic (EM) field in the plane holding the transmitting antenna elements. When treating the antenna elements as ideal point sources, the EM field is written as

$$f_{TX}(x, y) = \sum_{m=1}^M \sum_{n=0}^{N-1} e^{j2\pi m n / N} \delta(x - x_n, y - y_n), \quad (2)$$

where M is the total number of OAM modes transmitted, l_m is the integer OAM mode value, (x, y) are the coordinates on

the plane holding Tx antenna elements, $\delta(x,y)$ is the 2-dimensional Dirac delta function, j has imaginary units, x_n and y_n are given by $(x_n, y_n) = (R_{TX} \cos(2\pi n/N), R_{TX} \sin(2\pi n/N))$ and they represent the locations of each Tx antenna element. Next, we use the circular aperture function, which represents the size of thin lens given by

$$a(x', y') = \begin{cases} 1 & \text{if } x'^2 + y'^2 \leq R_L^2 \\ 0 & \text{if otherwise} \end{cases}, \quad (3)$$

where R_L is lens radius, and (x', y') are the coordinates on the plane holding the lens. Using the thin-lens formula, (2), and (3), we obtain the closed-form expression of the Fresnel diffraction pattern at the Rx position as

$$f_{RX}(X, Y) = C e^{-j\pi(X^2+Y^2)/\lambda d_2} \sum_{m=1}^M \sum_{n=0}^{N-1} e^{j2\pi m n/N} \pi R_L^2 \frac{2J_1\{R_L \cdot r_n(X, Y)\}}{R_L \cdot r_n(X, Y)}, \quad (4)$$

where (X, Y) are the coordinates on the plane holding the Rx antenna elements, λ is wavelength, $J_1(\cdot)$ is a Bessel function of the first kind, C is a complex constant containing all relevant factors such as attenuation, phase shift and $r_n(X, Y)$ is

$$r_n(X, Y) = \frac{2\pi}{\lambda d_1} \sqrt{\left(\frac{d_1}{d_2} X + x_n\right)^2 + \left(\frac{d_1}{d_2} Y + y_n\right)^2}. \quad (5)$$

4. Numerical Results

In this section, we numerically analyze the diffraction pattern of (4). In order to validate effectiveness of the proposed method, we compare it with conventional UCA [4]. Calculation parameters are shown in Table. 1.

First, we confirm the generation of OAM modes on the RX position (i.e. XY -plane in Fig. 2) by observing a rotating *phase front*, which is the defining feature of OAM beams [4]. Fig. 3(a) is a visualization of the phase of an OAM mode ($l_1=3$). The circle marked in Fig. 3(a) indicates the configured position of Rx antenna elements. From Fig. 3(a), the rotating phase front is observed on the Rx plane. Also, Fig. 3(b) shows the phase transition along the circle marked in Fig. 3(a). Obviously, the phase shift is periodic, and the number of periods in one revolution equals the OAM mode value, $l_1=3$. The result shows that the UCA Rx can obtain the exact phase profile of the OAM mode, which is necessary for separating multiplexed OAM modes.

Next, we evaluate beam divergence. The degree of beam divergence is evaluated from beam radius defined as the distance from the origin to the radial position of maximum intensity. Fig. 4 plots beam radius versus OAM mode. While the beam radius linearly expands with OAM mode value in the conventional approach, the radius changes little in the proposed approach up to $l_1=4$. Also, for $l_1 \geq 2$, the proposal yields smaller beam radii. The result shows that the proposed method can reduce beam divergence.

We also compare the intensity distribution on the Rx position. Figs. 5(a) and 5(b) show intensity distributions of OAM mode ($l_1=3$) for the proposed and conventional method respectively. The plotted values are log-normalized by dividing the total energy in $1m \times 1m$ grid. The proposed method yields an energy concentration around the Rx center. On the other hand, the conventional one scatters the power. This shows that proposed method can also reduce side lobes.

5. Conclusion

This paper proposed an antenna and lens arrangement method based on well-known optical imaging theory. We numerically analyzed the diffraction pattern at the Rx position. We confirmed that the OAM beam can be properly generated on the receiver plane. Also, we confirmed that the proposed method can reduce the impact of beam divergence as well as energy loss due to side lobes compared to the conventional UCA.

References

- [1] Y. Yan, *et al.* "High-capacity millimeter-wave communications with orbital angular momentum multiplexing.", *Nat. Commun.*, Vol. 5, p. 4876, 2014.
- [2] A. Honda, *et al.* "Development of wireless communications technologies for future multi-gigabit data transmission", in *Proc. of APMC.*, pp. 483-485, 2014.
- [3] F. Eslampanahi, *et al.* "4-Gbps uncompressed video transmission over a 60-GHz orbital angular momentum wireless channel", *IEEE wireless commun. lett.*, vol. 2, no. 2, pp.223-225, 2013.
- [4] S. Mohaghegh, *et al.* "Orbital angular momentum in radio –a system study", *IEEE trans. Antennas propag.*, vol. 58, no. 2, pp. 565-572, 2010.
- [5] T. Yuan, H. Wang, Y. Qin, and Y. Cheng, "Electromagnetic vortex imaging using uniform concentric circular arrays", *IEEE antennas and wireless propag. Let.*, Vol. 15, pp. 1024-1027, 2016.
- [6] M. Andersson, *et al.*, "Orbital angular momentum modes do not increase the channel capacity in communication links," *New J. Phys.* 17, 043040, 2015.
- [7] M. J. Padgett, *et al.* "Divergence of an orbital-angular-momentum-carrying beam upon propagation," *New J. Phys.*, 17, 023011, 2015.

Table. 1 Calculation parameters

Parameter	Value
Number of Arrays : N	24
Wavelength : λ	0.0050 m (60 GHz)
Radius of TX UCA : R_{TX}	0.025 m
Radius of RX UCA : R_{RX}	0.15 m
Radius of lens : R_L	0.10 m
Separation distance : z_L	3.5 m
Total number of OAM mode : M	1

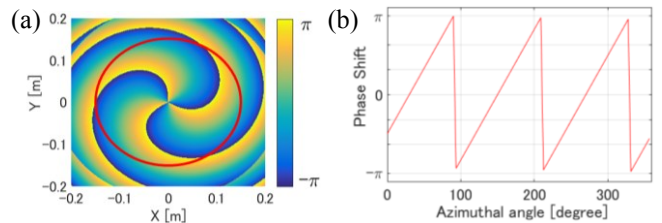


Fig.3 Phase of OAM mode ($l_1=3$); (a) represented in XY -plane, (b) along marked in Red circle of Fig. 3(a).

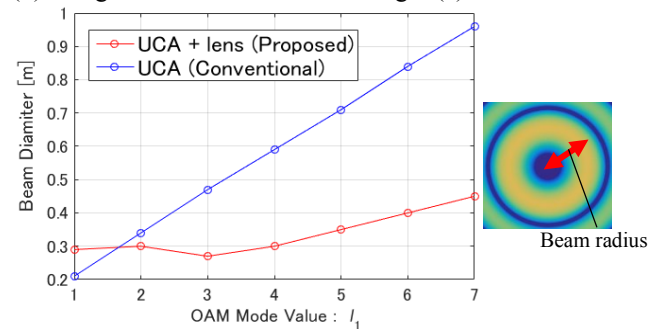


Fig.4 Comparison of beam radius. Cross marks indicate conventional UCA. Circles indicate proposed method.

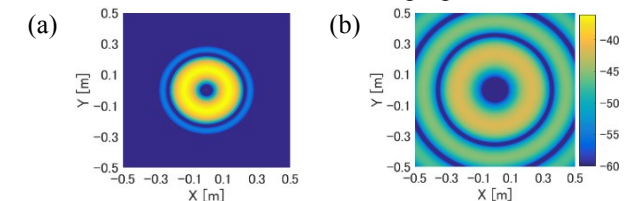


Fig.5 Intensity distributions of OAM mode ($l_1=3$) for; (a) Proposed method, (b) UCA.